BJR|Open https://doi.org/10.1259/bjro.20180020

Received: 20 August 2018 | Revised: 13 December 2018 | Accepted: 10 January 2019

Cite this article as:
Tate CJ, Mollee PN, Miles KA. Combination bone marrow imaging using positron emission tomography (PET)-MRI in plasma cell dyscrasias: correlation with prognostic laboratory values and clinicopathological diagnosis. *BJR Open* 2019; **1**: 20180020.

ORIGINAL RESEARCH

Combination bone marrow imaging using positron emission tomography (PET)-MRI in plasma cell dyscrasias: correlation with prognostic laboratory values and clinicopathological diagnosis

[1]COURTNEY J TATE, MBBS, BSc (Hons), PhD, [2]PETER N MOLLEE, MBBS, MMedSc, FRACP, FRCPA and [3]KENNETH A MILES, MBBS, MSc, MD, FRCP, FRANZCR

[1]Princess Alexandra Hospital, Royal Brisbane and Women's Hospital, University of Queensland, QLD, Australia
[2]Institute of Nuclear Medicine, University College London, QLD, Australia
[3]Princess Alexandra Hospital, University of Queensland, QLD, Australia

Address correspondence to: Dr Courtney J Tate
E-mail: *courtmodra@hotmail.com*

Objective: This prospective observational study of positron emission tomography (PET)-MRI findings in 16 consecutive newly diagnosed patients with a plasma cell dyscrasia describes and compares MRI-detected myeloma lesions with ^{18}F-fludeoxyglucose PET-avid myeloma lesions, and correlates quantitative imaging findings to a range of biochemical and prognostic parameters.
Methods: Simultaneously acquired whole body PET and MRI images were evaluated qualitatively for the presence of focal or generalised abnormalities of bone marrow (BM) on either modality. Quantitative analysis comprised mean standardised uptake values (SUVmean) and fractional water content of the BM measured from PET and chemical shift MRI images of the second to fourth lumbar vertebrae.
Results: Final diagnoses comprised symptomatic myeloma (n = 10), asymptomatic myeloma (n = 4) and monoclonal gammopathy of uncertain significance (n = 2). 8/10 patients with symptomatic myeloma demonstrated BM abnormalities on qualitative assessment of MRI compared to 4/10 on PET. BM SUVmean inversely correlated with serum albumin (r = 0.57, p = 0.017). BM water fraction correlated with trephine cellularity and blood platelet count (r = 0.78, p = 0.00039 and r = 0.61, p = 0.0013 respectively). BM water fraction correlated with SUVmean in patients with low plasma cell burden (r = 0.91, p = 0.0015) but not in patients with high plasma cell burden (r = 0.18, p = 0.61).
Conclusion: PET-MRI shows promise in both morphological and functional multiparametric quantitative assessment of myeloma.
Advances in knowledge: For the first time, multiparametric imaging in myeloma has been shown to predict BM abnormalities and correlate with known biochemical prognostic markers, moving PET-MRI beyond simple diagnostic applications into potential prognostic and treatment selection applications.

INTRODUCTION

MRI is recommended by the International Myeloma Working Group (IMWG) as the imaging modality of choice in asymptomatic myeloma patients, in staging of solitary plasmacytomas, and in myeloma patients with suspected neurological or soft tissue involvement.[1,2] MRI, over any other imaging modality, has a higher sensitivity for detecting axial skeleton lesions, and detects marrow infiltration by myeloma cells much earlier than myeloma related bone destruction detected by CT, positron emission tomography-CT (PET-CT) or x-ray.[3,4] In current IMWG guidelines, patients with greater than one focal lesion of diameter >5 mm on MRI are considered to have symptomatic disease requiring therapy. However, MRI, CT and X-ray have the disadvantage of detecting persistent non-viable lesions after treatment, even in patients achieving a complete remission.[5,6] In comparison, ^{18}F-fludeoxyglucose (FDG)-PET has the capacity to reveal metabolic marrow changes, and in combination with low dose CT has been shown to predict survival and may provide for a better definition of complete remission.[7,8]

Hybrid PET-MRI imaging platforms have recently become available with approval from the FDA for clinical use in 2012. Simultaneous PET and MRI acquisition has particular advantage over other imaging modalities for solid

malignancies with bony metastasis.[9] In myeloma, simultaneous PET and MRI acquisition theoretically combines highly sensitive MRI with PET-avidity to detect active lesions, potentially providing superior diagnostic accuracy and response assessment. PET-MRI also offers opportunities for multiparametric quantitative imaging with the potential to extract a range of quantifiable features for the assessment of disease severity and/or change during treatment. To our knowledge simultaneous PET-MRI acquisition in myeloma has been evaluated only once previously, and myeloma bone involvement was defined as PET-avid lesions rather than IMWG recommended MRI-detected bone lesions, with the purpose of the study being to compare PET-MRI-avidity to PET-CT-avidity.[10] Moreover, the relationship between quantitative PET-MRI parameters and myeloma disease status is currently unknown. Our present prospective observational study uses a Siemens Biograph MMR PET/3T MRI hybrid imaging system in 16 consecutive newly diagnosed patients with a plasma cell dyscrasia, to describe and compare MRI-detected myeloma lesions with FDG-PET-avid myeloma lesions, as well as correlate quantitative imaging findings to a range of clinical, biochemical and prognostic parameters.

METHODS

Study population

During 2015 and 2016, 16 consecutive newly diagnosed patients with a plasma cell dyscrasia from Princess Alexandra Hospital, Queensland, Australia were evaluated. The study was conducted in accordance with the Declaration of Helsinki and formed part of a non-interventional research programme seeking to identify prognostic imaging biomarkers, for which approval was granted by the local ethics committee who waived the need to obtain consent in individual patients.

Prior to initiating therapy all patients had baseline laboratory values collected, a bone marrow aspirate and trephine (BMAT), and a PET-MRI of either the axial skeleton or whole body. Patients were diagnosed according to the IMWG criteria[1] and staged according to the International Staging System (ISS)[11] and the Revised ISS (R-ISS).[12] Cytogenetic abnormalities on marrow aspirate sample were used to calculate R-ISS after performing fluorescence *in situ* hybridisation for one or 1p copy number abnormalities, 13 or 13q deletion, translocation of t(4;14) and deletion of 17p. BMAT analysis included blinded assessment by two haematologists of marrow cellularity, and plasma cell percentage using CD138 immunohistochemistry, with the average percentage being reported.

Patients excluded from this report included those who could not have a MRI for practical reasons, patients who needed urgent or immediate treatment, and patients likely to have monoclonal gammopathy of uncertain significance (MGUS) based on biochemical markers and clinical assessment prior to imaging and/or BM biopsy results. Despite attempting to exclude MGUS patients using these criteria, 2 of the 16 study participants had a final diagnosis of MGUS.

Image acquisition

Simultaneous FDG-PET/3T MRI images were acquired using a Siemens (Erlangen, Germany) Biograph mMR system comprising a 3 T MR scanner with an axial spatial resolution of 4.3 mm at 1 cm and 5.0 mm at 10 cm from the transverse field of view (FOV), a maximum sensitivity of 13.8 kcps/MBq at the centre of the FOV, and an axial FOV of 25.8 cm. Patients had fasted for at least 4 h with their serum glucose confirmed to be <10 mmol l^{-1} prior to intravenous administration of FDG (5MBq/kg to a maximum of 400 MBq). Images were acquired from the skull vertex to the feet at 60 min after radiotracer administration (5 min per bed position). MRI acquisitions included T_1 weighted Dixon acquisitions with chemical-shift imaging (CSI),[13] along with T_2 and short-tau inversion recovery (STIR) sequences. The MRI acquisition parameters are summarized in Table 1. PET images were reconstructed using ordered subset expectation maximization with 3 iterations and 21 subsets.

IMAGE EVALUATION

Qualitative analysis

A dual-trained radiologist/nuclear physician assessed each MRI and PET for BM involvement. On each modality, BM appearances were categorised as (1) normal marrow pattern; (2) focal abnormalities consisting of localized areas of high signal on STIR combined with low signal or iso-intensity to normal bone marrow on T_1 weighted images, and/or increased radiotracer uptake on FDG-PET; (3) variegated abnormalities consisting of innumerable small disease foci on a background of normal BM ("salt and pepper" appearance), and (4) diffuse abnormalities defined as normal BM completely replaced by abnormal BM signal, according to the IMWG PET and MRI diagnostic criteria.[2]

QUANTITATIVE ANALYSIS:

BM water fraction was chosen as the quantitative MRI parameter,[14] and CSI used to evaluate BM water content by analysis of in-phase (IP) images, in which the fat and water signals are additive, and opposed-phase (OP) images, in which fat and water

Table 1. Summary of MRI acquisition parameters

Sequences	Orientation	TR (ms)	TE (ms)	Slice thickness (mm)	Pixel size (mm)	FOV (mm)
T_1 VIBE DIXON[a]	Axial	3.85	1.24/2.46	3	1.3	500
T_2 HASTE	Axial	1300	912	5	1.3	400
STIR	Coronal	3500	54	5	1.2	450

FOV, field of view; STIR, short-tau inversion recovery; TE, echo time; TR, repetition time.
[a]also used for attenuation correction

signals cancel as described previously.[15–17] Using co-registered PET and MR images, a single operator blinded to the clinico-pathological data constructed regions of interest (ROIs) within the L2, L3 and L4 vertebrae at mid-vertebral level. ROI size was as large as vertebrae allowed, but avoiding partial volume effects. The iliac crest was not used due to possibility of recent bone marrow biopsy(ies) affecting tissue architecture, and because this would involve analysis of a single smaller region rather than the average of three larger ROI. FDG uptake was expressed as mean standardised uptake value (SUVmean) and BM fractional water content determined from CSI were measured in each ROI with values averaged between L2 and L4. Vertebrae containing focal lesions on PET or MRI (myeloma deposit or incidental lesions such as haemangiomata) were excluded from this analysis.

STATISTICAL ANALYSIS

Correlations between qualitative and quantitative PET-MRI findings and patient baseline laboratory values of haemoglobin (Hb), creatinine (Cr), corrected calcium (CCa), albumin, β2-microglobulin, ISS, R-ISS, and BM cellularity and BM plasma cell percentage were assessed using the Spearman Rank-Correlation test. "Low" and "high" plasma cell burden were defined as patients with a percentage of plasma cells in BM trephine below and above the median plasma cell percentage respectively.

RESULTS

Study population characteristics are outlined in Table 2 with final diagnoses for the 16 patients comprising symptomatic myeloma (n = 10), asymptomatic myeloma (n = 4) and MGUS (n = 2).

Qualitative analysis

Analysis of MRI images in symptomatic myeloma and asymptomatic myeloma patients for BM involvement showed 6/14 (43%) patients had normal marrow pattern (asymptomatic myeloma n = 4, myeloma n = 2), 4/14 (29%) patients had focal abnormalities, 3/14 (21%) patients had focal and variegated abnormalities, and 1/14 (7%) patient had variegated abnormalities. No patients had diffuse marrow abnormalities.

Analysis of PET images in myeloma and asymptomatic myeloma patients showed 5/14 (36%) patients had PET-avid bone disease. Therefore, of the eight patients with MRI-detected bone disease, only five were PET-avid (Table 3). Figure 1 depicts visual analysis from simultaneously acquired PET-MRI images in two patients with MRI-detected bone disease: one who was PET-negative and another who was PET-avid. Neither modality detected qualitative marrow abnormalities in patients with asymptomatic myeloma or MGUS.

Quantitative analysis

MRI marrow water fraction showed a significant positive correlation with trephine cellularity (r = 0.78, p = 0.00039) (Figure 2a) , but not trephine plasma cell burden (r = 0.4957, p = 0.05). PET marrow SUVmean inversely correlated with serum albumin (r = 0.57, p = 0.017) (Figure 2b) but showed no correlation with trephine cellularity or plasma cell burden. MRI marrow water fraction correlated with PET marrow SUVmean in patients with lower plasma cell burden (r = 0.91, p = 0.0015) (Figure 2c) but not in patients with higher plasma cell burden (r = 0.18, p = 0.61) (Figure 2d). MRI marrow water fraction and PET marrow SUVmean showed no correlation to Hb, Cr, CCa, β2-microglobulin, ISS, and R-ISS.

Table 2. Study population characteristics

	Number (%)
Diagnosis	
Myeloma	10 (63)
Asymptomatic myeloma	4 (25)
MGUS	2 (12)
Age, year	
Median	69
Range	35–82
Sex	
Male	11 (70)
Female	5 (30)
Subtype	
IgG	11 (69)
IgA	1 (6)
Light chain	4 (25)
Bone marrow plasma cells[a]	
Median	(48)
Range	(5-80)
ISS[a]	
Stage I	5 (36)
Stage II	5 (36)
Stage III	4 (28)
R-ISS[a,b]	
Stage I	2 (14)
Stage II	9 (64)
Stage III	1 (7)

ISS, international staging system;MGUS, monoclonal gammaopathy of uncertain significance; R-ISS, revised-ISS.
[a]MGUS patients (n = 2) were not included in these analysis.
[b]Two patients had insufficient sample for cytogenetics and R-ISS could not be determined.

DISCUSSION

Myeloma bone disease represents a major cause of morbidity in myeloma. Appropriate use of imaging techniques to identify both bony disease and extramedullary foci at diagnosis is critical and forms a standard component of diagnostic assessment. Combined PET-MRI acquisition provides the opportunity to obtain highly sensitive MRI images together with PET-avidity in a single exam. We have shown that of the eight patients with MRI-detected bone disease, only five were PET-avid, indicating MRI images are superior to PET-avidity for identifying patients with myeloma bone disease when acquired using a hybrid PET-MRI imaging platform. In addition, patients 1 and 4 had

Table 3. Patient characteristics

Patient	Age	Sex	Diagnosis	Paraprotein	Hb	Cr	CCa	ISS	R-ISS	PC (%)	C (%)	MRI	PET	FWC	SUV
1	58	M	Myeloma	β + κ IgA 22 g l^{-1}	134	79	2.7	II	II	50	50	V	Yes-mild	0.593	0.865
2	67	M	Myeloma	κ IgG 65 g l^{-1}	84	128	2.2	II	II	80	45	*V* + Focal	Yes	0.552	2.300
3	69	M	Myeloma	κ IgG 47 g l^{-1}	97	107	2.69	II	II	50	45	*V* + Focal	Yes	0.566	6.400
4	76	M	Myeloma	λ IgG 19 g l^{-1}	141	79	2.49	I	I	35	45	*V* + Focal	Yes*	0.513	2.035
5	82	M	Myeloma	κ IgG 47 g l^{-1}	96	163	2.38	III	III	60	25	Focal	Yes	0.229	2.020
6	44	F	Myeloma	κSFLC 890 ml l^{-1} (ratio 210)	132	81	2.44	I	I	70	70	Focal	Neg	0.807	1.640
7	35	M	Myeloma	κ IgG 31 g l^{-1}	134	75	2.26	II	II	45	40	Focal	Neg	0.338	1.700
8	82	M	Myeloma	λ IgG 19 g l^{-1}	103	272	2.27	III	II	50	35	Focal	Neg	0.609	1.625
9	73	M	Myeloma	κ IgG 31 g l^{-1}	86	113	2.35	III	II	75	80	Neg	Neg	0.681	1.960
10	69	F	Myeloma	κ IgG 23 g l^{-1}	98	45	2.3	I	*	65	30	Neg	Neg	0.121	0.635
11	79	M	AS	λ IgG 8 g l^{-1}	92	368	2.88	III	II	10	30	Neg	Neg	0.354	1.793
12	60	F	AS	κ IgG 28 g l^{-1}	125	87	2.43	II	II	27.5	40	Neg	Neg	0.550	2.757
13	59	M	AS	κ IgG 26 g l^{-1}	124	105	2.3	I	*	10	20	Neg	Neg	0.151	0.725
14	80	F	AS	λSFLC 1600 mg l^{-1} (ratio 0.04)	116	78	2.33	I	II	15	40	Neg	Neg	0.165	1.423
15	66	M	MGUS	λSFLC 140 mg l^{-1} (ratio 0.2)	153	78	2.25	NA	NA	5	25	Neg	Neg	0.386	2.050
16	80	F	MGUS	λSFLC 1900 mg l^{-1} (ratio 0.01)	117	103	2.39	NA	NA	5	25	Neg	Neg	0.260	1.353

, unable to be determined; AS, aymptomatic myeloma; C (%), marrow cellularity on trephine; CCa, corrected calcium (umol/L); Cr, creatinine (umol/L); FWC, fractional water content determined from MRI T1-weightedDixon chemical-shift imaging (CSI); Hb, haemaglobin (g/L); ISS, International Staging System; NA, not applicable; Neg, negative; PC (%), plasma cell percentage on trephine; R-ISS, Revised-ISS; λSFLC, λ serum free light chain; SUV, mean standardised uptake value on PET images; V, variegated; Yes, mild avidity for larger lesions, negative for smaller lesions; kSFLC, κ serum free light chain.

[a]patient also had AL amyloid

Figure 1. Visual analysis from simultaneously acquired PET-MRI Images in 2 patients. (a) In patient 1, MRI bone marrow involvement shows a variegated ('salt and pepper') pattern not apparent on PET. (b) In patient 3, both PET and MRI detected focal marrow abnormalities in upper humeri, spine (prominent L1 deposit), pelvis and upper femurs.

only low-grade PET-avidity, suggesting PET underestimates the extent and burden of disease. This agrees with previous findings comparing MRI and PET-CT images acquired separately.

MRI-detected myeloma lesions that are not FDG avid are thought to represent indolent or quiescent disease, however in our cohort, patients 6, 7 and 8 had MRI-detected, PET-negative bone involvement, with biochemically active disease necessitating therapy. While the SUV of myeloma lesions depicted on PET-MRI has been reported to be significantly lower than respective values on PET-CT, PET-MRI sensitivity when compared to PET-CT is 94%.[10] Alternative explanations for MRI-positive PET-negative myeloma bone lesions in biochemically active disease includes PET-negativity due to low hexokinase-2 expression[18] or low plasma cell proliferation indices in these patients. Malignant plasma cells have a relatively low proliferation index compared to other malignancies, with a proliferation index comparable to MGUS and asymptomatic myeloma patients in some myeloma

Figure 2. Significant correlations between quantitative PET and quantitative MRI analysis, clinicopathological features and prognostic laboratory values. (a) MRI marrow water fraction directly correlates with trephine cellularity. (b) PET marrow maximal SUV inversely correlates with serum albumin. (c) MRI marrow water fraction correlates with PET BM maximal SUV in patients with lower plasma cell burden. (d) MRI marrow water fraction does not correlate with PET BM maximal SUV in patients with higher plasma cell burden. BM, bone marrow; PET, positron emission tomography; SUV, standardised uptake values.

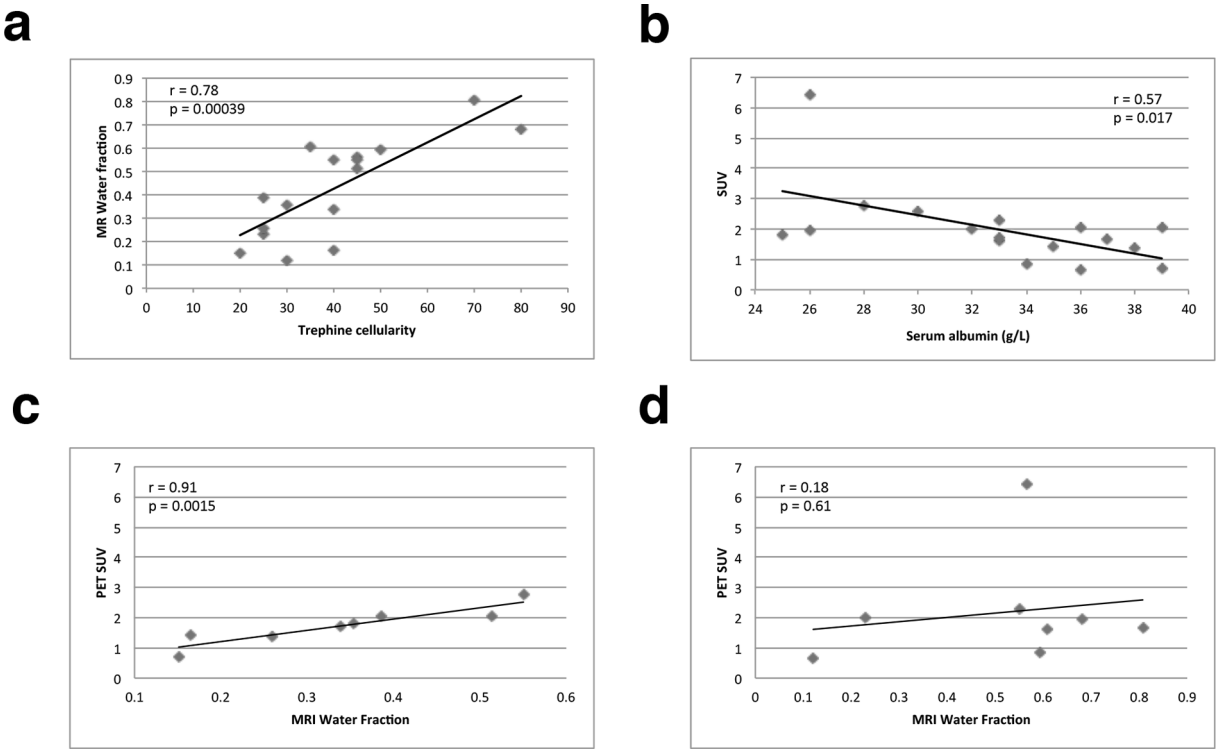

patients.[19] However, if a high plasma cell proliferation index is present, this is known to be a poor prognostic indicator in newly diagnosed myeloma and in biochemically stable disease with minimal residual plasma cell burden.[20,21] This apparent variability in plasma cell proliferation and corresponding metabolism may also underlie the loss of correlation between BM and water fraction and SUVmean in patients with higher plasma cell burden. It is therefore possible that MRI-detected, PET-negative bone disease and/or high BM water fraction with low SUVmean at diagnosis may reflect a low plasma cell proliferation index, and a better prognostic subgroup of myeloma.

Current guidelines do not stipulate imaging as mandatory for monitoring response to therapy, except for following plasmacytomas, extraosseous disease and non-secretory myeloma. Myeloma bone lesions persist on X-ray and CT even in patients achieving a complete response to therapy. Maximal SUV on PET-CT has been used to monitor response to therapy, with three or fewer lesions after Day 7 of induction therapy,[7] and suppression of lesions after induction[8] and after completing treatment[22] good prognostic indicators, whereas a maximal SUV greater than 4.2 after treatment correlating with relapsed disease.[23] Therefore, in patients with PET-avid disease at diagnosis, subsequent imaging with PET-MRI may provide a useful tool to assess response to therapy. However, due to our finding that a proportion of patients with MRI-detected bone disease are PET-negative at diagnosis, future studies using PET-MRI to assess treatment response need to confirm PET-avidity of individual patients/malignant clone(s) at diagnosis. Furthermore, consideration needs to be given to the potential for malignant plasma cells to evolve characteristics that result in less rapid proliferation, and hence reduced PET-avidity, which could be misinterpreted as a response to therapy.

Our comparison of quantitative hybrid PET-MRI features to clinical, biochemical and prognostic parameters revealed correlations that may be useful in clinical practice. In particular, BM SUVmean inversely correlating to the known myeloma prognostic marker albumin suggests prognostic biomarkers may be derived from multiparametric PET-MRI. Despite that fact that CSI with MRI detects both intra- and extracellular water, our analysis has also demonstrated a significant correlation between BM water content and cellularity on trephine. Hence, in the absence of significant bone oedema, MRI marrow water fraction can provide a surrogate marker for marrow cellularity. Marrow cellularity, traditionally determined by BM biopsy, forms a part of diagnostic criteria for a variety of marrow disorders, including aplastic anaemia or hypoplastic MDS. Marrow cellularity is also of interest in peripheral blood cytopenias post-chemotherapy, which can reflect either heavy marrow involvement with persistent disease, or alternatively hypoplastic marrow where malignant cells and normal haematopoiesis/red marrow are replaced by fatty marrow. MRI marrow water fraction may provide a useful adjunct to determine marrow cellularity in patients not fit for BM biopsy, or where the disease is inherently patchy making BM biopsy susceptible to sampling error. Indeed, our finding that MRI marrow water fraction is not able to predict the burden of BM plasma cell involvement on trephine in myeloma patients possibly reflects the patchy nature of myeloma bone involvement and inherent limitations of BM trephine in determining overall marrow plasma cell burden. In addition to cellularity and proliferation, combination PET-MRI could characterise additional features such as hypoxia and perfusion. This information could potentially improve tumour biology profiling and prognostification.[24] The added value of multiparametric imaging for prognosis and treatment selection can move PET-MRI beyond simple diagnostic applications and so facilitate cost-effective utilisation of this hybrid modality.[25]

Alternative MRI techniques can be implemented on PET-MRI for quantitative assessment of bone marrow. Most notably, diffusion-weighted imaging (DWI) with measurement of apparent diffusion coefficient (ADC) has shown promise in multiple myeloma.[26,27] Although pre-dating current experience with DWI, the most recently published imaging guidelines from the International Myeloma working group advocate T_1 and STIR images,[28] and inclusion of additional DWI sequences would extend the PET-MRI imaging time beyond that required for acquisition of PET data. Given the high cost of PET-MRI systems, such protocols are relatively uneconomic as the device is being used for MRI alone for a significant period of time. Furthermore, standard whole-body DWI acquisitions used in PET-MRI are subject to distortion artefacts, which may result in misregistration between PET and MRI data sets. A recent study recorded 19 distortion artefacts when using standard DWI sequences for PET-MRI in a series of 20 oncological patients.[29] The frequency of artefacts increased when a simultaneous multislice technique was used to reduce acquisition time. Multishot echo planar imaging can reduce anatomical distortion during DWI but such techniques require even longer image acquisitions, further exacerbating the economic challenges. By using Dixon sequences for CSI, the bone marrow water fraction can be determined from the same acquisition as the T1 images required for morphological assessment. CSI measurements of water fraction have also recently been shown to benefit from superior reproducibility compared to ADC values.[16]

While the main aim of this study was to evaluate the feasibility of PET-MRI to detect myeloma bone involvement at diagnosis, we acknowledge its major limitation of a small sample size. This may explain the lack of correlation between quantitative imaging features and BM plasma cell burden, or prognostic markers other than albumin. Future work in larger cohorts assessing these parameters should also consider PET-MRI pre- and post-treatment to determine if the perceived advantage of monitoring for changes in PET-avidity can predict patient response to therapy, which is currently determined using biochemical criteria alone in the majority of patients. As treatments for myeloma evolve resulting in improved outcomes for patients, detection of residual disease using sensitive methods not susceptible to sampling error is increasingly important, and novel methods such as hybrid PET-MRI may provide useful adjunctive information that contributes to optimal patient management.

CONCLUSION

PET-MRI shows promise not only in morphological and molecular assessment of myeloma at diagnosis, but also provides functional multiparametric quantitative information that reflects the heterogeneous tissue microenvironment, prognostic laboratory values and variable clinical phenotypes.

REFERENCES

1. Rajkumar SV, Dimopoulos MA, Palumbo A, Blade J, Merlini G, Mateos MV, et al. International myeloma Working Group updated criteria for the diagnosis of multiple myeloma. *Lancet Oncol* 2014; **15**: e538–48. doi: https://doi.org/10.1016/S1470-2045(14)70442-5
2. Dimopoulos M, Terpos E, Comenzo RL, Tosi P, Beksac M, Sezer O, et al. International myeloma Working Group consensus statement and guidelines regarding the current role of imaging techniques in the diagnosis and monitoring of multiple myeloma. *Leukemia* 2009; **23**: 1545–56. doi: https://doi.org/10.1038/leu.2009.89
3. Zamagni E, Nanni C, Patriarca F, Englaro E, Castellucci P, Geatti O, et al. A prospective comparison of 18F-fluorodeoxyglucose positron emission tomography-computed tomography, magnetic resonance imaging and whole-body planar radiographs in the assessment of bone disease in newly diagnosed multiple myeloma. *Haematologica* 2007; **92**: 50–5. doi: https://doi.org/10.3324/haematol.10554
4. Giles SL, deSouza NM, Collins DJ, Morgan VA, West S, Davies FE, et al. Assessing myeloma bone disease with whole-body diffusion-weighted imaging: comparison with X-ray skeletal survey by region and relationship with laboratory estimates of disease burden. *Clin Radiol* 2015; **70**: 614–21. doi: https://doi.org/10.1016/j.crad.2015.02.013
5. Bannas P, Hentschel HB, Bley TA, Treszl A, Eulenburg C, Derlin T, et al. Diagnostic performance of whole-body MRI for the detection of persistent or relapsing disease in multiple myeloma after stem cell transplantation. *Eur Radiol* 2012; **22**: 2007–12. doi: https://doi.org/10.1007/s00330-012-2445-y
6. Wahlin A, Holm J, Osterman G, Norberg B. Evaluation of serial bone x-ray examination in multiple myeloma. *Acta Med Scand* 1982; **212**: 385–7. doi: https://doi.org/10.1111/j.0954-6820.1982.tb03234.x
7. Usmani SZ, Mitchell A, Waheed S, Crowley J, Hoering A, Petty N, et al. Prognostic implications of serial 18-fluoro-deoxyglucose emission tomography in multiple myeloma treated with total therapy 3. *Blood* 2013; **121**: 1819–23. doi: https://doi.org/10.1182/blood-2012-08-451690
8. Bartel TB, Haessler J, Brown TL, Shaughnessy JD, van Rhee F, Anaissie E, et al. F18-fluorodeoxyglucose positron emission tomography in the context of other imaging techniques and prognostic factors in multiple myeloma. *Blood* 2009; **114**: 2068–76. doi: https://doi.org/10.1182/blood-2009-03-213280
9. Beiderwellen K, Huebner M, Heusch P, Grueneisen J, Ruhlmann V, Nensa F, et al. Whole-body [18F]FDG PET/MRI vs. PET/CT in the assessment of bone lesions in oncological patients: initial results. *Eur Radiol* 2014; **24**: 2023–30. doi: https://doi.org/10.1007/s00330-014-3229-3
10. Sachpekidis C, Hillengass J, Goldschmidt H, Mosebach J, Pan L, Schlemmer HP, et al. Comparison of (18)F-FDG PET/CT and PET/MRI in patients with multiple myeloma. *Am J Nucl Med Mol Imaging* 2015; **5**: 469–78.
11. Greipp PR, San Miguel J, Durie BG, Crowley JJ, Barlogie B, Blade J. International staging system for multiple myeloma. J Clin Oncol 2005;23:3412-20. Erratum in. *J Clin Oncol* 2005; **23**: 6281.
12. Palumbo A, Avet-Loiseau H, Oliva S, Lokhorst HM, Goldschmidt H, Rosinol L, et al. Revised international staging system for multiple myeloma: a report from international myeloma Working Group. *JCO* 2015; **33**: 2863–9. doi: https://doi.org/10.1200/JCO.2015.61.2267
13. Maas M, Akkerman EM, Venema HW, Stoker J, Den Heeten GJ. Dixon quantitative chemical shift MRI for bone marrow evaluation in the lumbar spine: a reproducibility study in healthy volunteers. *J Comput Assist Tomogr* 2001; **25**: 691–7. doi: https://doi.org/10.1097/00004728-200109000-00005
14. Takasu M, Tani C, Sakoda Y, Ishikawa M, Tanitame K, Date S, et al. Iterative decomposition of water and fat with ECHO asymmetry and least-squares estimation (ideal) imaging of multiple myeloma: initial clinical efficiency results. *Eur Radiol* 2012; **22**: 1114–21. doi: https://doi.org/10.1007/s00330-011-2351-8
15. Latifoltojar A, Hall-Craggs M, Rabin N, Popat R, Bainbridge A, Dikaios N, et al. Whole body magnetic resonance imaging in newly diagnosed multiple myeloma: early changes in lesional signal fat fraction predict disease response. *Br J Haematol* 2017; **176**: 222–33. doi: https://doi.org/10.1111/bjh.14401
16. Latifoltojar A, Hall-Craggs M, Bainbridge A, Rabin N, Popat R, Rismani A, et al. Whole-body MRI quantitative biomarkers are associated significantly with treatment response in patients with newly diagnosed symptomatic multiple myeloma following bortezomib induction. *Eur Radiol* 2017; **27**: 5325–36. doi: https://doi.org/10.1007/s00330-017-4907-8
17. Dreizin D, Ahlawat S, Del Grande F, Fayad LM. Gradient-echo in-phase and opposed-phase chemical shift imaging: role in evaluating bone marrow. *Clin Radiol* 2014; **69**: 648–57. doi: https://doi.org/10.1016/j.crad.2014.01.027
18. Schraml C, Schmid M, Gatidis S, Schmidt H, la Fougère C, Nikolaou K, et al. Multiparametric analysis of bone marrow in cancer patients using simultaneous PET/MR imaging: correlation of fat fraction, diffusivity, metabolic activity, and anthropometric data. *J Magn Reson Imaging* 2015; **42**: 1048–56. doi: https://doi.org/10.1002/jmri.24865
19. Yoo HJ, Hong SH, Kim DH, Choi JY, Chae HD, Jeong BM, et al. Measurement of fat content in vertebral marrow using a modified Dixon sequence to differentiate benign from malignant processes. *J Magn Reson Imaging* 2017; **45**: 1534–44. doi: https://doi.org/10.1002/jmri.25496
20. Rasche L, Angtuaco E, McDonald JE, Buros A, Stein C, Pawlyn C, et al. Low expression of Hexokinase-2 is associated with false-negative FDG-positron emission tomography in multiple myeloma. *Blood* 2017; **130**: 30–4. doi: https://doi.org/10.1182/blood-2017-03-774422
21. Greipp PR, Kyle RA. Clinical, morphological, and cell kinetic differences among multiple myeloma, monoclonal gammopathy of undetermined significance, and smoldering multiple myeloma. *Blood* 1983; **62**: 166–71.
22. Greipp PR, Lust JA, O'Fallon WM, Katzmann JA, Witzig TE, Kyle RA. Plasma cell labeling index and beta 2-microglobulin predict

survival independent of thymidine kinase and C-reactive protein in multiple myeloma. *Blood* 1993; **81**: 3382–7.

23. Steensma DP, Gertz MA, Greipp PR, Kyle RA, Lacy MQ, Lust JA, et al. A high bone marrow plasma cell labeling index in stable plateau-phase multiple myeloma is a marker for early disease progression and death. *Blood* 2001; **97**: 2522–3. doi: https://doi.org/10.1182/blood.V97.8.2522
24. Zamagni E, Nanni C, Mancuso K, Tacchetti P, Pezzi A, Pantani L, et al. PET/CT improves the definition of complete response and allows to detect otherwise unidentifiable skeletal progression in multiple myeloma. *Clin Cancer Res* 2015; **21**: 4384–90. doi: https://doi.org/10.1158/1078-0432.CCR-15-0396
25. Bailey DL, Pichler BJ, Gückel B, Barthel H, Beer AJ B. Combined PET/MRI: multi-modality multi-parametric imaging is here: summary report of the 4th International Workshop on PET/MR imagingTübingen, Germany. *Mol Imaging Biol* 2015; **2015**: 595–608.
26. Miles KA, Voo SA, Groves AM. Additional clinical value for PET/MRI in oncology: moving beyond simple diagnosis. *J Nucl Med* 2018; **59**: 1028–32. doi: https://doi.org/10.2967/jnumed.117.203612
27. Sachpekidis C, Mosebach J, Freitag MT, Wilhelm T, Mai EK, Goldschmidt H. Application of (18)F-FDG PET and diffusion weighted imaging (DWI) in multiple myeloma: comparison of functional imaging modalities. *Am J Nucl Med Mol Imaging* 2015; **12;5**: 479–92.
28. Pawlyn C, Fowkes L, Otero S, Jones JR, Boyd KD, Davies FE, et al. Whole-body diffusion-weighted MRI: a new gold standard for assessing disease burden in patients with multiple myeloma? *Leukemia* 2016; **30**: 1446–8. doi: https://doi.org/10.1038/leu.2015.338
29. Taron J, Schraml C, Pfannenberg C, Reimold M, Schwenzer N, Nikolaou K, et al. Simultaneous multislice diffusion-weighted imaging in whole-body positron emission tomography/magnetic resonance imaging for multiparametric examination in oncological patients. *Eur Radiol* 2018; **28**: 3372–83. doi: https://doi.org/10.1007/s00330-017-5216-y